Steel and Composite Structures, *Vol. 21*, *No. 4* (*2016*) *829-847*
DOI: http://dx.doi.org/10.12989/scs.2016.21.4.829

Study on flexural capacity of simply supported steel-concrete composite beam

Jing Liu [1], Fa-xing Ding [*1], Xue-mei Liu [2] and Zhi-wu Yu [1,3]

[1] *School of Civil Engineering*, *Central South University*, *Changsha*, *Hunan Province*, *410075*, *P.R. China*
[2] *School of Civil Engineering and Built Environment*, *Queensland University of Technology*, *Brisbane*, *QLD 4000*, *Australia*
[3] *National Engineering Laboratory for High Speed Railway Construction*, *Changsha*, *410075*, *P.R. China*

(*Received February 04*, *2016*, *Revised June 06*, *2016*, *Accepted June 17*, *2016*)

Abstract. This paper investigates the flexural capacity of simply supported steel-concrete composite I beam and box beam under positive bending moment through combined experimental and finite element (FE) modeling. 24 composite beams are included into the experiments and parameters including shear connection degree, transverse reinforcement ratio, section form of girder, diameter of stud and loading way are also considered and investigated. ABAQUS is employed to establish FE models to simulate the behavior of composite beams. The influences of a few key parameters, such as the shear connection degree, stud arrangement, stud diameter, beam length and loading way, on flexural capacity are discussed. In addition, three methods including GB standard, Eurocode 4, and Nie method are also used to estimate the flexural capacity of composite beams and also for comparison with experimental and numerical results. The results indicate that Nie method may provide a better estimation in comparison to other two standards.

Keywords: steel-concrete composite beam; flexural capacity; finite element; degree of shear connection

1. Introduction

Steel-concrete composite beams are broadly applied in civil buildings and bridges in recent years. This structure is composed of concrete slab and steel beam in order to utilize the material properties. Thus, its own high capacity, low self-weight, convenient construction than traditional steel or concrete structures. Flexural capacity being a vital parameter due to the great cross-section is used widely in practice. Currently, various methods recommended by different standards and scholars are available to estimate the flexural capacity of steel-concrete composite beams.

The shear connection of steel-concrete composite beam can be divided into full shear connection and partial shear connection in theory. The former can guarantee the bearing capacity. The latter reduces the number of the stud and benefits reinforcing bar colligation. Johnson (1994) established a formula to calculate the flexural capacity of partial shear connection of steel-concrete composite beams according to the degree of shear connection with linear interpolation method, which had adopted by the Eurocode 4. China code GB 50017 proposed a formula to calculate the

*Corresponding author, Professor, E-mail: dinfaxin@csu.edu.cn

http://www.techno-press.org/?journal=scs&subpage=6 ISSN: 1229-9367 (Print), 1598-6233 (Online)

flexural capacity of partial shear connection of steel-concrete composite beams according to the simplified plastic theory. Nie (Nie and Cai 2003) revised the partial shear connection formula established by Johnson (1994).

Both theoretical and experimental research on steel-concrete composite beam has been carried out in recent years. Salari (1999) researched the bond-slip in steel-concrete composite beam, which consider the nonlinear analysis of frame structures with composite floor systems, and the author presented three different composite beam elements to accounting the bond-slip effect. Zhao *et al.* (2012) have completed 2 full scale steel-concrete composite beams tests under monotonic positive bending. A macro-modeling approach was proposed for the nonlinear analysis of composite beams. Three different parameters, the compressive strength of concrete, the yield strength of the steel flanges and web, and the shear connection degree were applied to research the ultimate moment of composite beam. Souici *et al.* (2013) researched the behaviour of both traditionally connected and innovatively bonded steel–concrete composite beams. The full connection by shear studs was difficult to ensure a continuous transmission of shear force between the steel beam and the concrete slab. Kim *et al.* (2011) conducted experimental and analytical evaluations of the ultimate strength of composite structures with consideration of different degrees of shear connections. Hicks and Pennington (2015) presented the results from a reliability analysis on the resistance of composite beams in sagging bending which were designed according to Eurocode 4. It focused on the partial factors for the design resistance of composite beams in bending. Vasdravellis (Vasdravellis *et al.* 2015) presented an experimental and numerical study on the ultimate strength of steel–concrete composite beams subjected to the combined effects of sagging (or positive) bending and axial compression.

Other research on the composite beams such as the distortional buckling, long term behavior *etc* can also be found from references (Zhou *et al.* 2015, 2016, Selçuk and Metin 2013, Fan *et al.* 2010a, b).

Finite element method is a mainly analysis method for predicting the response of steel–concrete composite structures in the past few years. Wang and Chang (2013) presented a numerical study of axially loaded concrete-filled steel tubular columns with "T" shaped cross section (CFTTS) based on the ABAQUS software. Chang *et al.* (2014, 2015) investigated the performance of composite structures and rock structures by ABAQUS. Tao and Nie (2014) proposed a fiber beam-column model considering slab spatial composite effect for nonlinear analysis of composite frame systems. Mirza and Uy (2011) investigated the behavior of composite beam–column flush end-plate connections subjected to low-probability, high-consequence loading by ABAQUS. Geng *et al.* (2014) and Liu *et al.* (2014) researched the mechanical property of concrete-filled steel tubular (CFST) arch bridges by ABAQUS or OpenSees. A nonlinear finite element model was developed and found to be capable to accurately predict the nonlinear response and the combined strength of the tested composite beams by Vasdravellis (Vasdravellis *et al.* 2015). The model relies on the use of the commercial software ABAQUS.

The above mentioned literatures indicated that the steel-concrete composite beam generally perform well under flexural loadings. Some parameters, including shear connection degree, transverse reinforcement ratio, the diameter of stud, the section form of girder, and the loading condition, which influenced the flexural capacity of steel-concrete composite beams have not been thoroughly investigated through experimental study. Some other factors such as the stud in double row layout, beam span, the loading position and way, have not been discussed neither. Moreover, various countries' standard are not compared in a much wider range of factors covers FE results and tested ones.

Therefore, this paper aims to thoroughly investigate the flexural capacity of steel-concrete composite beams with respect to a few key influencing factors and evaluate the different methods in calculation of flexural capacity from different standards. More specifically, based on the theoretical, numerical and experimental research in our team (Ding *et al*. 2011, 2016), four objectives are included in this study: (1) To investigate the flexural capacity of 24 simply supported steel-concrete composite I beam and box beam subjected to positive bending moment through experimental study; (2) To establish FE models using ABAQUS program to simulate the flexural performance of the steel-concrete composite beams; (3) To conduct parametric study to investigate the effect of various factors on the flexural behavior of steel-concrete composite beams; (4) To compare and evaluate different methods including GB 50017, Eurocode 4 and Nie method with respect to the experimental results and numerical results from FEA on the flexural performance of steel-concrete composite beams.

2. Experimental study

2.1 Materials and specimens

24 steel-concrete composite beams were included into the experimental study. Cross section of girder is shown in Fig. 1. Composite test loading device is shown in Figs. 2~3. Detailed geometric properties and characteristics of the specimens are presented in Table 1. l is the length of the specimen, w_c is the width of the concrete slab, h_c is the depth of concrete, w_s is the width of steel beam, h_s is the height of steel beam and d is the diameter of stud. ρ_{st} is ratio of transverse reinforcement of concrete slab, ρ_{sl} is ratio of longitudinal reinforcement of concrete slab. η is the degree of shear connection (by GB 50017 2003).

Before the beam testing, material testing was conducted to obtain the respective material properties. The cubic compressive strength f_{cu} of concrete and tensile coupon tests on steel plates are presented in Table 2. $f_{s,b}$ means the yield strength of steel, $f_{s,s}$ means the yield strength of stud, f_u means the ultimate strength of stud and f_{cu} represents the concrete compressive strength. Various

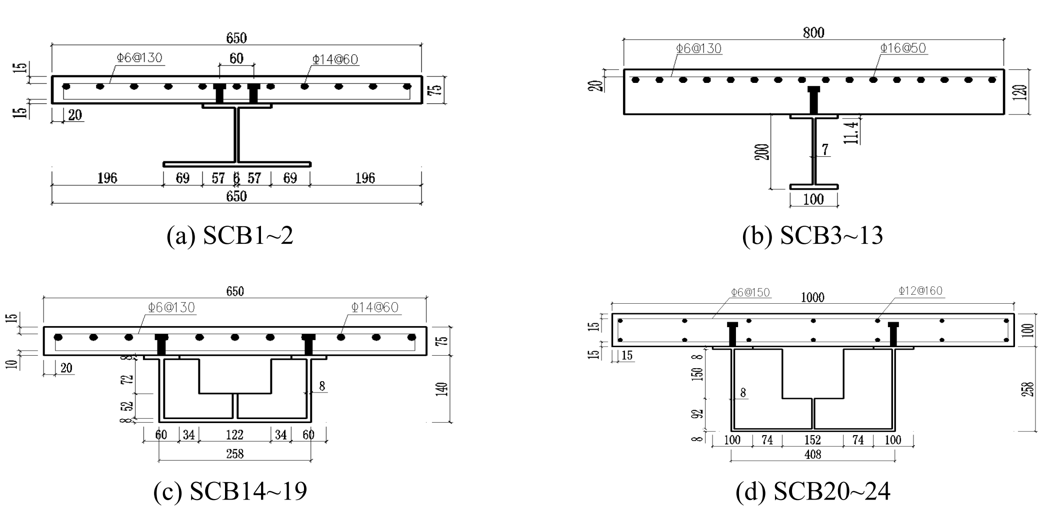

(a) SCB1~2 (b) SCB3~13

(c) SCB14~19 (d) SCB20~24

Fig. 1 Cross section details of the girder

(a) SCB1~2, 14~19

(b) SCB3~13

(c) SCB20~24

Fig. 2 Test setup on spot

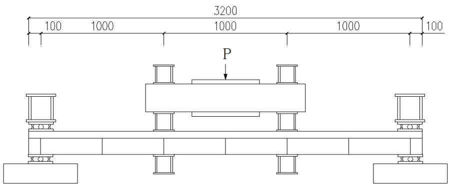

(a) SCB1~2, 14~19

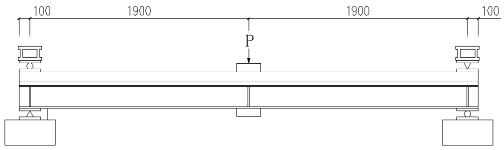

(b) SCB3~13

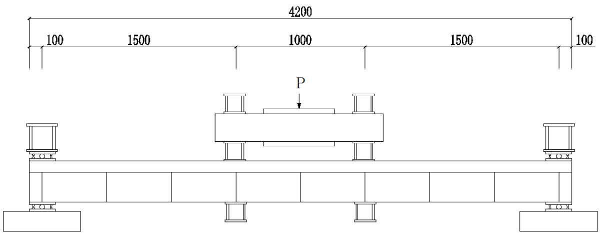

(c) SCB20~24

Fig. 3 Experimental setup for all specimens

Table 1 Geometric properties and characteristics of composite beams

No.	Loading mode	l/mm	w_c/mm	h_c/mm	w_s/mm	h_s/mm	d/mm	η	ρ_{st}/%	ρ_{sl}/%	M/kN
SCB1	dynamic cyclic	3000	650	75	258	140	13	0.85	0.62	3.47	156
SCB2	dynamic cyclic	3000	650	75	258	140	13	0.34	0.62	3.47	140
SCB3	dynamic cyclic	3800	800	120	200	200	16	1.86	0.32	2.51	206
SCB4	dynamic cyclic	3800	800	120	200	200	16	1.62	0.32	2.51	199
SCB5	dynamic cyclic	3800	800	120	200	200	16	1.32	0.32	2.51	179

Table 1 Continued

No.	Loading mode	l/mm	w_c/mm	h_c/mm	w_s/mm	h_s/mm	d/mm	η	ρ_{st}/%	ρ_{sl}/%	M/kN
SCB6	dynamic cyclic	3800	800	120	200	200	16	1.08	0.32	2.51	178
SCB7	dynamic cyclic	3800	800	120	200	200	16	0.84	0.32	2.51	168
SCB8	monotonic loading	3800	800	120	200	200	16	1.32	0.32	3.35	179
SCB9	monotonic loading	3800	800	120	200	200	16	1.32	0.32	2.93	187
SCB10	dynamic cyclic	3800	800	120	200	200	16	1.32	0.20	2.51	255
SCB11	dynamic cyclic	3800	800	120	200	200	16	1.32	0.43	2.51	261
SCB12	dynamic cyclic	3800	800	120	200	200	16	1.32	0.59	2.51	242
SCB13	dynamic cyclic	3800	800	120	200	200	16	1.32	0.78	2.51	273
SCB14	dynamic cyclic	3000	650	75	258	140	13	0.96	0.62	3.47	169
SCB15	dynamic cyclic	3000	650	75	258	140	13	0.66	0.62	3.47	163
SCB16	dynamic cyclic	3000	650	75	258	140	13	0.34	0.62	3.47	143
SCB17	dynamic cyclic	3000	650	75	258	140	13	0.96	0.62	1.89	163
SCB18	dynamic cyclic	3000	650	75	258	140	13	0.66	0.62	1.89	143
SCB19	dynamic cyclic	3000	650	75	258	140	13	0.34	0.62	1.89	138
SCB20	dynamic cyclic	4000	1000	100	408	258	13	0.98	0.38	1.58	546
SCB21	dynamic cyclic	4000	1000	100	408	258	16	1.01	0.38	1.58	560
SCB22	dynamic cyclic	4000	1000	100	408	258	19	1.00	0.38	1.58	572
SCB23	dynamic cyclic	4000	1000	100	408	258	16	0.70	0.38	1.58	506
SCB24	dynamic cyclic	4000	1000	100	408	258	16	1.32	0.38	1.58	584

Table 2 Properties of steel and concrete

No.	$f_{s,s}$/MPa	$f_{s,b}$/MPa	f_u/MPa	f_{cu}/MPa	E_s/MPa	No.	$f_{s,s}$/MPa	f_u/MPa	$f_{s,r}$/MPa	f_{cu}/MPa	E_s/MPa
SCB1	330	324	440	35.5	2.07×10^5	**SCB13**	350	480	380	40.8	2.02×10^5
SCB2	330	324	440	35.5	2.07×10^5	**SCB14**	330	440	453	35.5	2.01×10^5
SCB3	350	250	480	44.3	2.09×10^5	**SCB15**	330	440	453	35.5	2.01×10^5
SCB4	350	250	480	44.3	2.09×10^5	**SCB16**	330	440	453	35.5	2.01×10^5
SCB5	350	250	480	43.4	2.09×10^5	**SCB17**	330	440	453	35.5	2.01×10^5
SCB6	350	250	480	48.5	2.09×10^5	**SCB18**	330	440	453	35.5	2.01×10^5
SCB7	350	250	480	42.2	2.09×10^5	**SCB19**	330	440	453	35.5	2.01×10^5
SCB8	350	250	480	38.2	2.09×10^5	**SCB20**	330	440	440	43.7	2.01×10^5
SCB9	350	250	480	46.2	2.09×10^5	**SCB21**	350	460	440	43.7	2.01×10^5
SCB10	350	320	480	41.9	2.02×10^5	**SCB22**	350	455	440	43.7	2.01×10^5
SCB11	350	320	480	42.1	2.02×10^5	**SCB23**	350	460	440	43.7	2.01×10^5
SCB12	350	320	480	49.69	2.02×10^5	**SCB24**	350	460	440	43.7	2.01×10^5

grades of concrete are included in the study with concrete strength varing from 35.5 to 49.7 MPa. The tensile strengths of steel are 250 to 324 MPa as per design.

2.2 Testing system and method

Experiments on steel-concrete composite beams specimens were conducted in the National Engineering Laboratory for High Speed Railway Construction. 24 specimens were designed and tested in two scenarios. The first scenario used the monotonic loading mode and included two specimens labeled SCB8 and SCB9. The second scenario applied dynamic cyclic loading mode and included the remaining 22 specimens for testing.

2.3 Experimental results and discussion

Degree of shear connection is a key factor for the calculation of regarding the steel-concrete composite beams flexural capacity for various codes, therefore, its definition is presented here with the expression for the following analysis and discussion.

$$\eta = n / n_f \tag{1}$$

where n = actual number of shear connectors between intermediate point and the adjacent support. n_f = number of connectors for full shear connection. $n_f = V_s/V_u$. V_s is the entire horizontal shear at the interface between the steel beam and the concrete slab, which shall be taken as the lowest value according to the limit states of concrete crushing and tensile yielding of the steel section. V_u is the nominal strength of one stud shear connector. The definition of V_s and V_u may vary with the standards.

To further understand the factors influencing the flexural capacity of composite beams, this section is focusing to discuss such factors.

2.3.1 Factors influencing the flexural capacity

(1) The degree of shear connection

Relationship between flexural capacity and degree of shear connection is shown in Fig. 4. The contrast of SCB3~SCB7, SCB14~SCB16, SCB17~SCB19, shows that the higher the degree of shear connection, the larger the flexural capacity. The steel-concrete beam have good interaction behavior when η is high, which can minimize the deflection of composite beams under load, and guarantee the bearing capacity.

(2) The ratio of transverse reinforcement

Fig. 5 shows the relationship between the ratio of transverse reinforcement and flexural capacity. The SCB10~SCB13 contrast shows that the transverse reinforcement ratio between 0.20%~0.78%, has certain influence on the ultimate bearing capacity, the flexural capacity increased with the increase of transverse reinforcement ratio. This contributed to the higher transverse reinforcement ratio can enforce the confined effect, which ensure stud, steel beam and concrete work better so as to improve the flexural capacity of composite beams.

(3) The diameter of stud

The diameter of stud of SCB20~SCB22 are 13 mm, 16 mm, 19 mm, respectively. Those specimens own same degree of shear connection (about 1.2) because the number of stud was also changed. The bearing capacity of SCB21 is 2.6% than that of the SCB20 specimen, and the bearing capacity of SCB22 is 4.8% higher than the SCB20, which means that the bearing capacity has not been affected by the diameter of stud, as shown in Fig. 6.

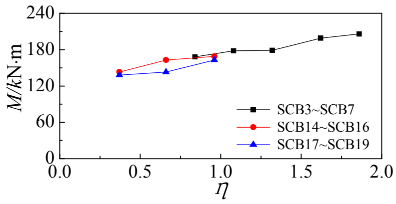

Fig. 4 Relationship between M and η

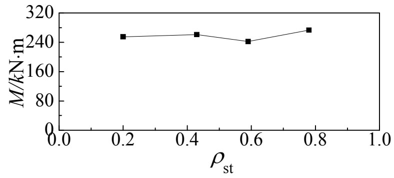

Fig. 5 Relationship between M and ρ_{st}

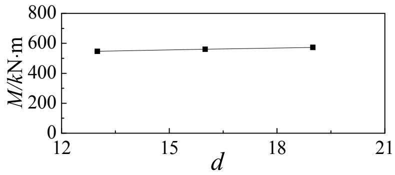

Fig. 6 Relationship between M and d

(4) The section form of girder

Table 1 and Fig. 1 show the relationship between the different section form and the flexural capacity. SCB2 is in I-shaped form and SCB16 is in box-shaped form. The flexural bearing capacity of SCB16 is 2.5% higher than that of SCB2, in other words, the box-shaped composite beam has a similar capacity compare I-shaped composite beam.

(5) The loading condition

The comparison of SCB5, SCB8 and SCB9 demonstrates that there is marginal difference in the flexural capacity obtained from dynamic cyclic loading condition and monotonic loading condition with the same degree of shear connection. The flexural capacity of SCB8 and that of SCB5 are the same, and the flexural capacity of SCB9 is only 4.8% lower than the SCB5 specimen, as shown in the Table 1.

3. Methods to estimate flexural capacity

3.1 GB standard

In Chinese national standard GB 50017-2003, the flexural capacity M of steel-concrete composite beams is expressed as follows:

(1) when $\eta \geq 1$, plastic neutral axis is in the concrete slab, namely $A_s f < w_c h_c f_c$

$$M = w_c x f_c y \tag{2a}$$

Where $x = Af/w_c f_c$

(2) when $\eta \geq 1$, plastic neutral axis is in the steel girder, that is $A_s f > w_c h_c f_c$

$$M = w_c h_{c1} f_c y_1 + A_c f y_2 \tag{2b}$$

Where $A_c = 0.5(A\text{-}w_c h_{c1} f_c/f)$.

(3) when $\eta < 1$

$$M = n_r V_u y_1 + 0.5(A_s f - n_r V_u) y_2 \tag{2c}$$

Where: $x = n_r N_v/(w_c f_c)$, $A_c = (Af–n_r N_v)/(2f)$
where h = depth of entire section. n_s = number of shear studs per row across flange. E_c = modulus of elasticity of concrete. A_c = area of concrete cross section, and A_s = area of steel cross section. f_c = compressive strength of concrete. y = distance of reinforcement to top fiber of steel beam. Other factors refer to GB 50017-2003.

3.2 Eurocode 4

A formula proposed by Johnson (1994) was adopted in the Eurocode 4 commentary, as follows

$$M = M_{ps} + \eta(M_{fu} - M_{ps}) \tag{3}$$

Where M_{fu} = Design value of the plastic resistance moment of the composite section with full shear connection, M_{ps} = Design value of the plastic resistance moment of the structural steel section. The calculation of shear connection refer to Eurocode 4.

3.3 Nie method

Nie proposed a simplified formula on the basis of Johnson (1994), as follows

$$M = M_{ps} + \eta^{0.5}(M_{fu} - M_{ps}) \tag{4}$$

The shear connection is same as GB 50017.

4. FE analysis

4.1 FE modeling

4.1.1 Material constitutive models

The material constitutive models of concrete suggested by Ding *et al*. (2011) are used for the model.

$$y = \begin{cases} \dfrac{kx + (m-1)x^2}{1 + (k-2)x + mx^2} & x \le 1 \\ \dfrac{x}{\alpha_1 (x-1)^2 + x} & x > 1 \end{cases} \tag{5}$$

where $y = \sigma/f_c$ and $x = \varepsilon/\varepsilon_c$ are the stress and strain ratio of the core concrete respectively. σ and ε are the stress and strain of the core concrete. $f_c = 0.4f_{cu}^{7/6}$ is the uniaxial compressive strength of concrete, where f_{cu} is the compressive strength of standard cubic concrete with 150 mm. ε_c is the strain corresponding with the peak compressive stress of concrete, where $\varepsilon_c = 383f_{cu}^{7/18} \times 10^{-6}$. The parameter k is the ratio of the initial tangent modulus to the secant modulus at peak stress. $m = 1.6(k-1)^2$ is a parameter that controls the decrease in the elastic modulus along the ascending branch of the axial stress-strain relationship. For a steel-concrete composite beam, parameter α_1 is determined by regression analysis as: $\alpha_1 = 2.5\times10^{-5}f_{cu}^{3}$.More information of the concrete model could be referred in Ding *et al*. (2011).

The Poisson ratio v_c of concrete is taken as 0.2. Eq. (5) is able to describe the stress-strain relationship of concrete with strengths ranging from 20 MPa to 140 MPa which has been validated by experimental results (Ding *et al*. 2011).

An elasto-plastic model, with consideration of Von Mises yield criteria, Prandtl-Reuss flow rule, and isotropic strain hardening, is used to des cribe the constitutive behavior of steel beam and longitudinal and transverse reinforcement bars. The expression for the stress-strain relationship of steel beam and rebar is as below (Ding *et al*. 2011).

$$\sigma_i = \begin{cases} E_s \varepsilon_i & \varepsilon_i \le \varepsilon_y \\ f_s & \varepsilon_y < \varepsilon_i \le \varepsilon_{st} \\ f_s + \zeta E_s (\varepsilon_i - \varepsilon_{st}) & \varepsilon_{st} < \varepsilon_i \le \varepsilon_u \\ f_u & \varepsilon_i > \varepsilon_u \end{cases} \tag{6}$$

where σ_i is the equivalent stress of steel beam or rebar; f_s is the yield strength; f_u is the ultimate strength and $f_u = 1.5f_s$; E_s is the elastic modulus, $E_s = 2.06\times10^5$ MPa; E_{st} is the strengthening modulus, which is described by $E_{st} = \zeta E_s$; ε_L is the equivalent strain; ε_y is the yield strain; ε_{st} is the strengthening strain; and ε_u is the ultimate strain, which is described by $\varepsilon_u = \varepsilon_{st} + 0.5f_s /(\zeta E_s)$, where $\varepsilon_{st} = 12\varepsilon_y$, $\varepsilon_u = 120\ \varepsilon_y$ and $\zeta = 1/216$.

The ideal elastic-plastic model is used for the studs in the concrete slabs, and the constitutive relation is as follows

$$\sigma_{is} = \begin{cases} E_{\mathrm{ss}} \varepsilon_{is} & \varepsilon_{is} \le \varepsilon_{\mathrm{ys}} \\ f_{\mathrm{ss}} + 0.01E_{\mathrm{ss}} (\varepsilon_{is} - \varepsilon_{\mathrm{ys}}) & \varepsilon_{\mathrm{ys}} < \varepsilon_{is} \le \varepsilon_{\mathrm{us}} = 21\varepsilon_{\mathrm{ys}} \\ f_{\mathrm{us}} = 1.2f_{\mathrm{ss}} & \varepsilon_{is} > \varepsilon_{\mathrm{us}} \end{cases} \tag{7}$$

where σ_{is} is the equivalent stress of stud; f_{ss} is the yield strength; f_{us} is the ultimate strength and $f_{us} = 1.2f_{ss}$; E_{ss} is the elastic modulus of stud as 2.06×10^5; ε_{is} is the equivalent strain, ε_{ys} is the yield strain and ε_{us} is ultimate strain of stud.

The stiffness of spring element is defined by load-slip curves and is used to simulate the shear stud. The well-known formula proposed by Ollgaard *et al*. (1971) that has been widely used in the literature.

$$V / V_u = (1 - e^{-0.71s})^{0.4} \tag{8}$$

where s is the average slip, V is shear capacity per stud. For a slip up to 5 mm, V reaches 99% of the ultimate load V_u. When the longitudinal, lateral and vertical stiffness adopt the Eq. (8) in this paper, nice results can be obtained.

4.1.2 Model stills

FE models are established by ABAQUS program (Hibbitt 2003), which is extensively adopted to analyze the composite structures and rock structures (Chang *et al*. 2014, 2015). FE models are established by ABAQUS. Four-node reduced integral format shell elements (S4R) are employed to

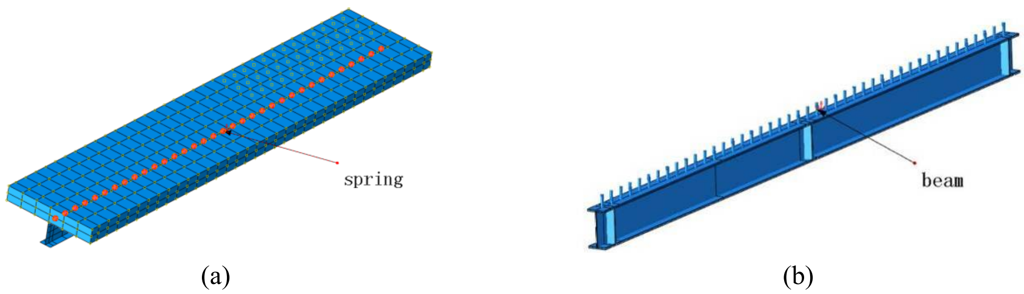

Fig. 7 Simplified FE models for steel-concrete composite beams using (a) spring elements; and (b) beam elements for studs

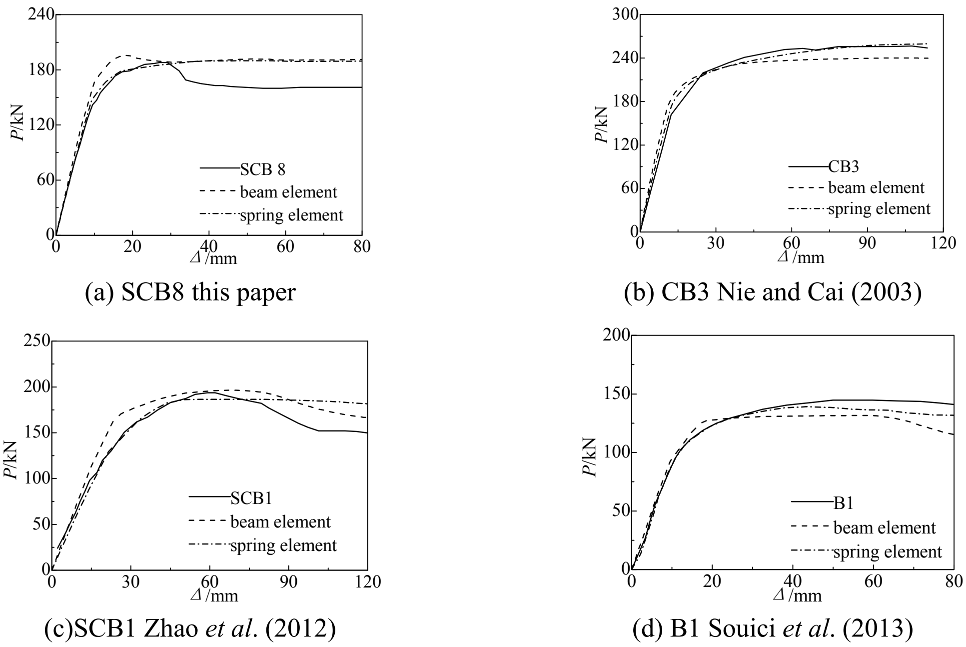

Fig. 8 Comparison between calculated and tested load deformation curve of steel-concrete composite beam

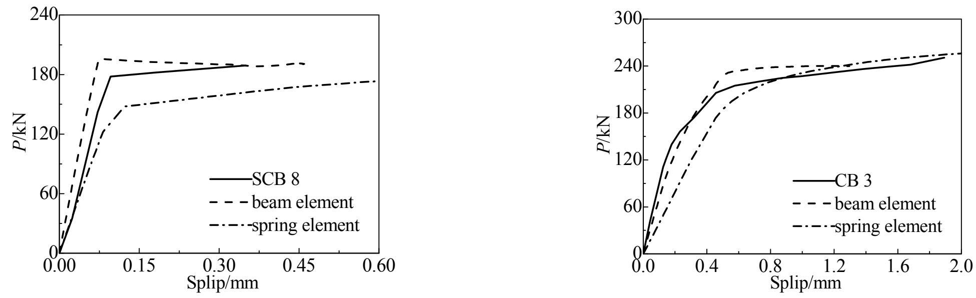

(a)SCB8 this paper (b) CB3 Nie *et al*.(2003)

Fig. 9 Comparison between calculated and tested load-end slip of composite steel-concrete beam of steel-concrete composite beam

model the steel beams. Concrete are modeled by eight-node brick elements (C3D8R). Reinforcement bars in specimens are modeled by the truss element T3D2, as truss element has been found to be effective and accurate in simulating the reinforcement in steel-concrete composite beams according to Ding *et al*. (2011).

In the FE model shown in Fig. 7(b), beam element (B31) is used to model the studs, and the studs are embedded in the concrete slab. The stiffness of the beam elements to represent the nonlinear load-slip relationship is then computed by ABAQUS.

The structured meshing technique is adopted. Mesh convergence studies are first performed to ensure that the FE mesh is sufficiently fine to give accurate results and the selected meshed models used for modelling are shown in Fig. 7. The type of contact between the steel and concrete is defined as surface to surface and coulomb friction model between concrete and steel is adopted for simulation. In the tangential direction, a friction coefficient of 0.5 is used for analysis. The sliding formulation is finite sliding, and a hard contact is defined in the normal direction. The boundary of the steel-concrete composite beam is simply supported as in the FE model.

Typical load-deflection curves of the specimens obtained from the FEA in comparison with the experimental results are shown in Fig. 8. The curves of slips at beam end versus load are shown in Fig. 9. Good agreement between experimental and FE modeling results are found in the elastic stage, and in the elastic-plastic stage and failure stage, the curve from FEA and the measured curve appeared with certain deviation. The simplified FE modeling approach using springs or beam elements can provide satisfactory modeling results for the experimental scenarios investigated.

4.2 Flexural capacity from FEA

For FEA, 34 groups of experimental data on steel-concrete composite beams are included for model validation and analysis.

M is the measured values of flexural capacity, M_{11} is the flexural capacity by spring element computing method. M_{12} is the flexural capacity by beam element computing method. M_2 is the flexural capacity by Eq. (2). M_3 is the flexural capacity by Eq. (3). M_4 is the flexural capacity by Eq. (4). The experimental results are compared with the predicted results using different methods including FEA, Eqs. (2), (3), and (4).

Table 3 shows comparison between simulated results and test results of steel-concrete composite beam. The average M/M_{11} ratio is 1.031 with a coefficient of variation at 0.089 for

Table 3 Comparison between Eqs. (2), (3), (4) results and tested ones

No.	Source of the specimens	Total number of specimens	Characteristic value	Spring element	Beam element	Eq. (2)	Eq. (3)	Eq. (4)
				M/M_{11}	M/M_{12}	M/M_2	M/M_3	M/M_4
1	this paper	24	Average	1.012	1.026	1.108	1.141	0.995
			Coefficient of variation	0.051	0.054	0.090	0.087	0.111
2	Nie and Cai 2003	4	Average	0.992	0.981	1.172	1.204	1.063
			Coefficient of variation	0.066	0.125	0.108	0.134	0.103
3	Salari 1999	1	Average	0.983	0.842	1.187	1.235	1.061
			Coefficient of variation	/	/	/	/	/
4	Zhao *et al.* 2012	2	Average	1.019	1.048	1.341	1.355	1.114
			Coefficient of variation	0.045	0.062	0.017	0.024	0.004
5	Souici *et al.* 2013	3	Average	1.268	1.359	1.534	1.655	1.410
			Coefficient of variation	0.049	0.034	0.152	0.163	0.140
6	All above	34	Average	1.031	1.046	1.169	1.209	1.049
			Coefficient of variation	0.089	0.118	0.150	0.165	0.156

spring element. The average M/M_{12} ratio is 1.046 with a coefficient of variation at 0.118 for beam element. Such findings indicate that the FE simulation results are very close to the experimental results.

4.3 Parametric study

From Section 4.2, it can be seen that the FE models can accurately simulate the flexural capacity for the steel-concrete composite beams. In this section, parametric studies are conducted to investigate the dominant factors on the flexural capacity. In addition, comparison study is also conducted between the FEA results and the standard results. Spring element is used for FEA in the following study with the reasons addressed as follows. Firstly, spring element can increase the computing efficiency for FEA. Secondly, spring element can simulate the stud stiffness value accurately in each direction, which is important for the simulation as the stud stiffness reflects the stud mechanical properties on the steel-concrete composite beams under sagging moment.

4.3.1 Influence of shear connection degree

Fig. 10 shows the geometric properties of steel-concrete composite beam, which loaded in mid-span, steel-concrete composite beam depth-span ratio, beam size, concrete wing size values are according to specification GB 50017. For convenient analysis, there is no longitudinal reinforcement in concrete slab. The span is 12 m. The stud is arranged in a single row layout, the stud diameter is 19 mm and its yield strength and ultimate strength are 350 MPa and 455 MPa respectively. There are 6 types of material combination groups in total for steel-concrete composite beam models: (1) Q235 steel paired with C30 and C40 concrete, (2) Q3455 steel paired with C40 and C50 concrete, (3) Q420 steel paired with C50 and C60 concrete. In total there are 43 cases for study.

Fig. 11 shows M-η relationship of steel-concrete composite beams under different degree of

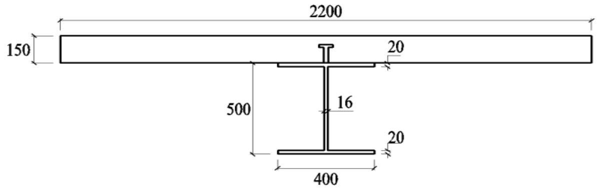

Fig. 10 Geometric properties of steel-concrete composite beam

shear connection. Relationships between *M* and *η* for Q345 matching C40 example are also obtained from three different methods, GB 50017, Eurocode 4, and Nie method are compared with the FEA results. It is found that, the shear connection degree has significant impact on flexural capacity of steel-concrete composite beams. *M* is increased with the increase of *η* value, but this phenomenon is not obvious when the connection degree is more than 1.

4.3.2 Influence of other factors

(1) Stud in double row layout

In this investigation, stud yield strength and ultimate strength, beam size and span, and stud diameter are the same as those defined in Section 4.1. In this analysis, two groups of composite beams are studied, with one group using Q235 steel and C30 concrete and the other using Q420 steel and C50 concrete. Fig. 12 demonstrates the relationship between *η* and *M* when stud is arranged in a double row layout. It can be seen that, the double row stud arrangement has little influence on flexural capacity of steel-concrete composite beams. *M*-*η* relationship of composite beam with Q235 steel and C30 concrete obtained from GB 50017, Eurocode 4, and Nie method are also presented in Fig. 12, respectively in comparison to the FEA results.

(2) The diameter of stud

In this investigation, stud yield strength and ultimate strength, beam size and span, and number of shear studs per row across flange are the same as those defined in Section 3.1 In this analysis, two groups of composite beams are studied, with one group using Q235 steel and C30 concrete and the other using Q420 steel and C50 concrete. The stud diameters are 16 mm, 22 mm, 25 mm respectively. Fig. 13 illustrates the relationship between *η* and *M*. It can be found that, diameter of stud has little influence on flexural capacity of steel-concrete composite beams. *M*-*η* relationship of composite beam with Q235 steel and C30 concrete obtained from GB 50017, Eurocode 4, and Nie method are also presented in Fig. 13, respectively in comparison to the FEA results.

(3) The loading position and way

In this investigation, stud yield strength and ultimate strength, beam size and span, and the diameter of stud are the same as those defined in Section 3.1. In this analysis, two groups of composite beams are studied, with one group using Q235 steel and C30 concrete and the other using Q420 steel and C50 concrete. The concentrate loading positions are 1/4, 1/3, 5/12 of beam span, and uniformly distributed loading is also adopted. Fig. 14 shows the relationship between *η* and *M*, it is found that, the loading position and way has few influence on flexural capacity of steel-concrete composite beams. Relationship between *M* and *η* of 3 kinds methods are selected from the Q235 matching C30 example. *M*-*η* relationship of composite beam with Q235 steel and C30 concrete obtained from GB 50017, Eurocode 4, and Nie method are also presented in Fig. 14 respectively in comparison to the FEA results.

(4) Span

In this investigation, stud yield strength and ultimate strength, and the diameter of stud are the same as those defined in Section 3.1. In this analysis, two groups of composite beams are studied, with one group using Q235 steel and C40 concrete and the other using Q345 steel and C40 concrete. The span are 4 m, 8 m, 16 m, 20 m respectively. Figs. 15(a)~(d) shows the relationship between η and M. It is found that, M is increased with the increase of η value in different beam

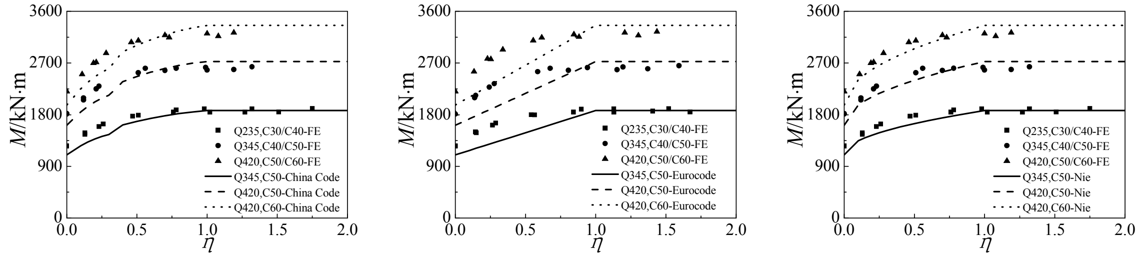

(a) (b) (c)

Fig. 11 The relationship of M-η: (a) Comparison between GB 50017 and FEA results; (b) Comparison between Eurocode 4 and FEA results; (c) Comparison between Nie method and FEA results

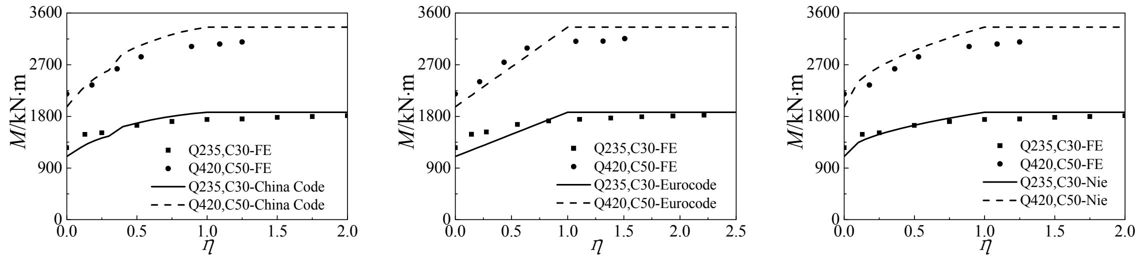

(a) (b) (c)

Fig. 12 Influence of double row stud to relationship of M-η: (a) Comparison between GB 50017 and FEA results; (b) Comparison between Eurocode 4 and FEA results; (c) Comparison between Nie method and FEA results

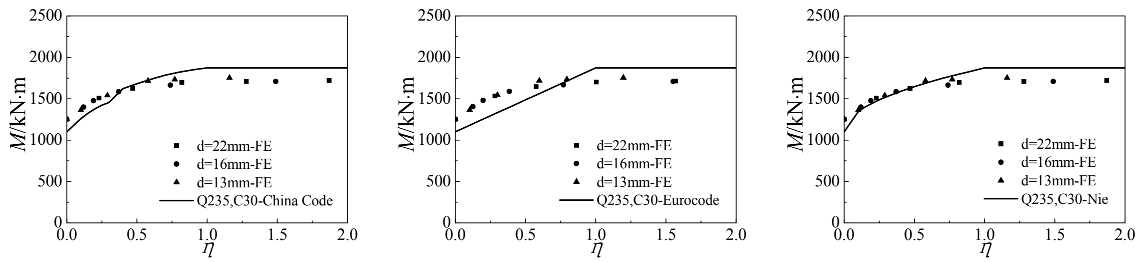

(a) (b) (c)

Fig. 13 Influence of stud diameter to relationship of M-η: (a) Comparison between GB 50017 and FEA results; (b) Comparison between Eurocode 4 and FEA results; (c) Comparison between Nie method and FEA results span. M-η relationship of composite beam with Q345 steel and C40 concrete obtained from GB 50017, Eurocode 4, and Nie method are also presented in Fig. 15 respectively in comparison to the FEA results.

The parameters of steel concrete composite beam considered in the parametric study include concrete strength from C30 to C60, steel strength from Q235 to Q420, stud row layout-single or double, stud diameter from 16 mm to 25 mm, stud yield strength and ultimate strength-350 MPa and 455 MPa respectively, beam span from 4 m to 20 m, shear span ratio from 1/4 to 1/2, load

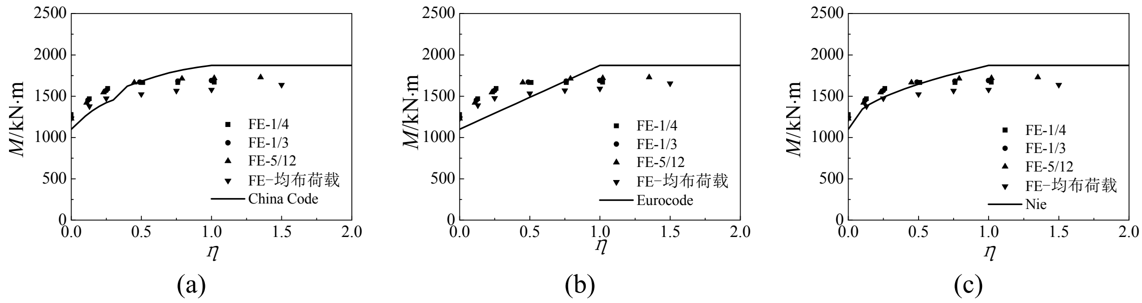

Fig. 14 Influence of Loading position and mode to relationship of M-η: (a) Comparison between GB 50017 and FEA results; (b) Comparison between Eurocode 4 and FEA results; (c) Comparison between Nie method and FEA results

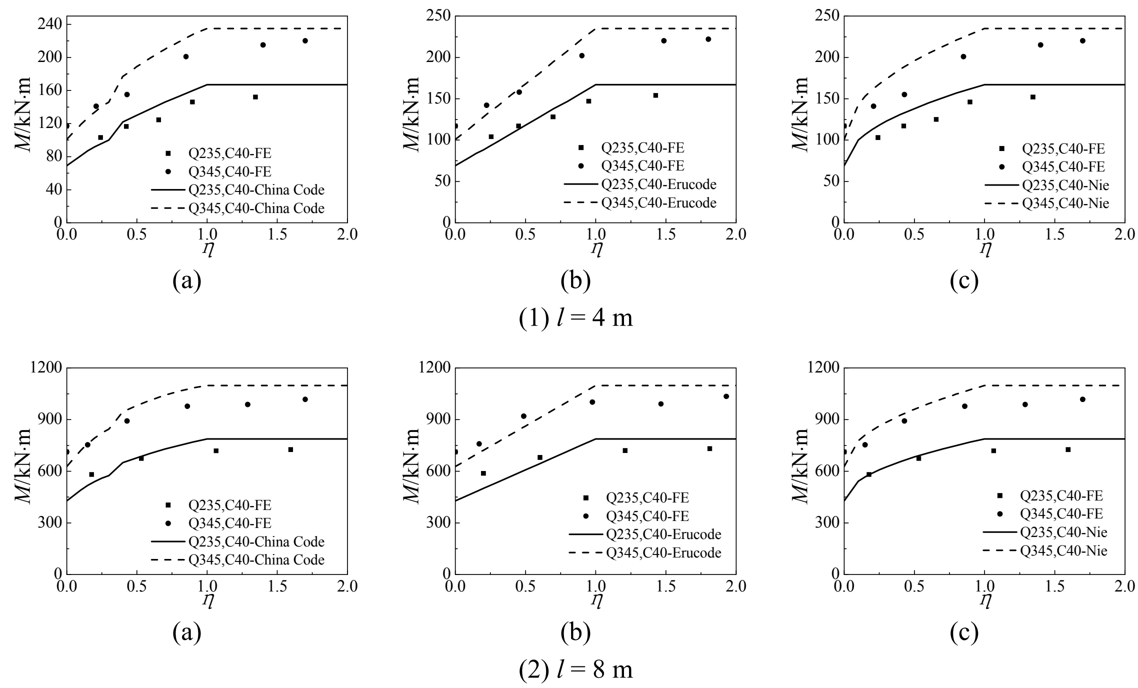

Fig. 15 Influence of beam length to relationship of M-η: (a) Comparison between GB 50017 and FEA results; (b) Comparison between Eurocode 4 and FEA results; (c) Comparison between Nie method and FEA results

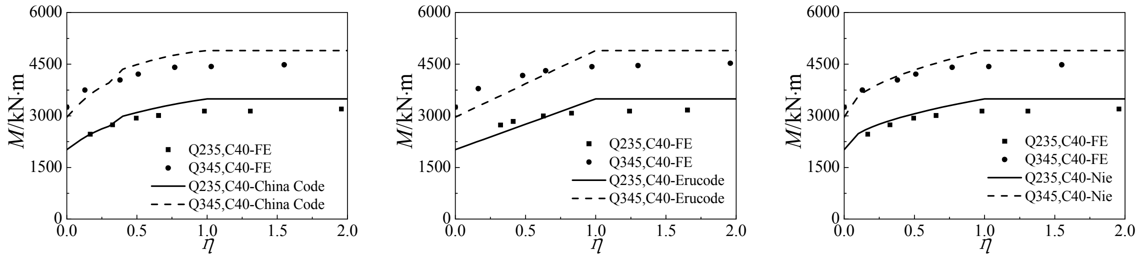

(a) (b) (c)

(3) l = 16 m

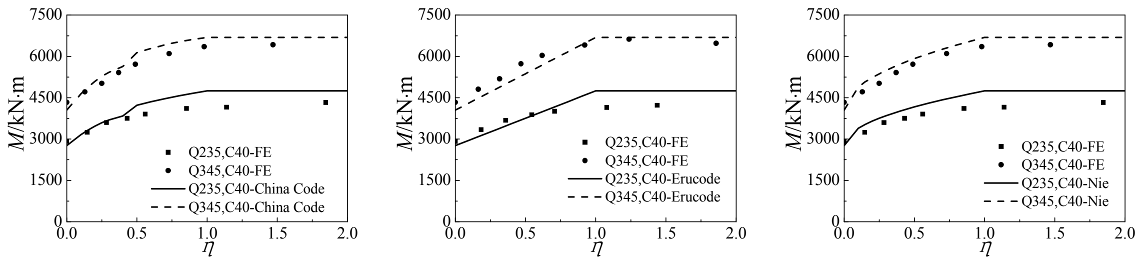

(a) (b) (c)

(4) l = 20 m

Fig. 15 Continued

Table 4 Parameters of composite steel-concrete beam

l/m	w_c /m	h_c /m	w_s /m	h_s /m	d /mm	$f_{s,s}$ /MPa	f_u /MPa	f_{cu} /MPa	$f_{s,b}$ /MPa
4	0.8	0.08	0.1	0.2	16	350	455	C40	235,345
8	1.5	0.12	0.25	0.4	16	350	455	C40	235,345
12	2.2	0.15	0.4	0.5	19	350	455	C30,C40, C50,C60	235,345,420
16	2.4	0.16	0.45	0.75	19	350	455	C40	235,345
20	2.6	0.2	0.5	0.9	22	350	455	C40	235,345

ways including point loading and uniformly distributed loading. The overall geometry of specimens in this parametric investigation, namely the geometry of concrete slab, steel beam, headed studs, and strength of materials, is shown in Table 4.

4.3.3 Summary and discussion

The experimental results are compared with the predicted results using different methods including Eqs. (2), (3), and (4), as shown in Table 3. The average M/M_2 ratio is 1.169 with a coefficient of variation at 0.150 for Eq. (2). The average M/M_3 ratio is 1.209 with a coefficient of variation at 0.165 for Eq. (3). The average M/M_4 ratio is 1.049 with a coefficient of variation at 0.156 for Eq. (4). The Eqs. (2),(3) provide more conservative results compare the test results, this contribute to the value of f_c is lesser than the Nie method.

FEA results by ABAQUS are compared with Eqs. (2), (3), (4), as shown in Table 5. In practical the shear connection degree is generally greater than 0.5, therefore the connection degree greater

Table 5 Comparison between Eqs. (2), (3), (4) results and FE ones

No.	Type	Total number of specimens	Characteristic value	Eq.(2) M_{FE}/M_2	Eq.(3) M_{FE}/M_3	Eq.(4) M_{FE}/M_4
1	Material	43	Average	1.053	1.081	1.014
			Coefficient of variation	0.111	0.140	0.075
2	Row of stud	17	Average	0.955	0.991	0.952
			Coefficient of variation	0.109	0.165	0.093
3	Diameter of stud	19	Average	1.009	1.023	0.978
			Coefficient of variation	0.085	0.183	0.109
4	Load pattern	26	Average	1.011	1.062	0.992
			Coefficient of variation	0.102	0.142	0.096
5	Span	55	Average	0.997	1.005	0.960
			Coefficient of variation	0.175	0.223	0.193
6	Total	160	Average	1.011	1.036	0.981
			Coefficient of variation	0.134	0.181	0.134

than 0.5 is considered in the validation. In Table 5, M_{FE} is the measured values of flexural capacity by ABAQUS. The average M_{FE}/M_2 ratio is 1.011 with a coefficient of variation at 0.134. The average M_{FE}/M_3 ratio is 1.036 with a coefficient of variation at 0.181. The average M_{FE}/M_4 ratio is 0.981 with a coefficient of variation at 0.134. In Table 3, three methods to calculate the flexural capacity are choose the same value of f_c as in FEA analysis, so three methods are in good agreement with the FE results, which means the plastic analysis method is feasible for calculating the flexural capacity of steel-concrete composite beams.

In summary, the calculate method by Nie has brief expression and high calculation precision, which has wider applicability than the other two formulas.

5. Conclusions

This paper has presented a combined experimental and numerical study of the flexural capacity of steel-concrete composite beam in comparison to the current widely used standard methods. From this study, the following conclusions can be drawn.

(1) The experimental results suggest that the bigger the connection degree is, the larger the flexural capacity will be. The flexural capacity increased with the increased of transverse reinforcement ratio, and the box-shaped composite beams have a high capacity than I-shaped composite beam. The bearing capacity has not been affected by the diameter of stud and the loading condition.

(2) Both beam element and spring element could be used to model the stud and achieved good agreement with the test results. However, in comparison, the spring element method has higher accuracy and faster computational speed than beam element method.

(3) Based on parametric analysis with spring element, it is found η is the main factor influencing the flexural capacity. The greater the degree of shear connection, the larger the flexural capacity, whereas after the degree of shear connection reaching 1, the growth of

flexural capacity is not significant. Other factors including stud in double row layout, stud diameter, beam span, loading location and way, had little impact on the flexural capacity.

(4) With both experimental research, parametric analysis and FEA, comparison for three calculation methods about flexural capacity of steel-concrete composite beams have been conducted. The results indicate that Nie method may provide a better estimation in comparison to the other two standard methods.

Acknowledgments

This research work is financially supported by the National Key Technology R&D Program, Grant No. 2011BAJ09B02 and the National Natural Science Foundation of China, Grant No. 51578548.

References

Chang, X., Luo, X.L., Zhu, C.X. and Tang, C.A. (2014), "Analysis of circular concrete-filled steel tube support in high ground stress conditions", *Tunn. Undergr. Sp. Tech.*, **43**(3), 41-48.

Chang, X., Wang, J.H., Zhang, Z.H. and Tang, C.A. (2015), "Effects of interface behavior on fracture spacing in layered rock", *Rock Mech. Rock Eng.*, **49**(5), 1733-1746.

Ding, F.X., Ying, X.Y., Zhou, L.C. and Yu, Z.W. (2011), "Unified calculation method and its application in determining the uniaxial mechanical properties of concrete", *Front. Archit. Civ. Eng. China*, **5**(3), 381-393.

Ding, F.X., Liu, J. and Liu, X.M. (2016), "Flexural stiffness of steel-concrete composite beam under positive moment", *Steel Compos. Struct., Int. J.*, **20**(6), 1369-1389.

Eurocode 4, European Standard (2004), Design of composite steel and concrete structures, Part 1.1: General rules and rules for buildings-General rules, EN 1994-1-1.

Fan, J.S., Nie, J.G. and Li, Q.W. (2010a), "Long-term behavior of composite beams under positive and negative bending (I)-Experimental study", *J. Struct. Eng.*, **136**(7), 849-857.

Fan, J.S., Nie, X. and Li, Q. (2010b), "Long-term behavior of composite beams under positive and negative bending. II: Analytical study", *J. Struct. Eng.*, **136**(7), 858-865.

GB 50017-2003, China Standard (2003), Code for design of steel structures; China Planning Press, Beijing, China.

Geng, Y., Wang, Y.Y., Ranzi, G. and Wu, X. (2014), "Time-dependent analysis of long-span, concrete-filled steel tubular arch bridges", *J. Bridge Eng.*, **19**(4), 111-122.

Hibbitt, Karlson & Sorensen Inc. (2003), ABAQUS/standard User's Manual, Version 6.4.1., Pawtucket, RI, USA.

Hicks, S.J. and Pennington, A. (2015), "Partial factors for the design resistance of composite beams in bending", *J. Construct. Steel Res.*, **105**(2), 74-85.

Liu, C.Y., Wang, Y.Y., Wang, W. and Wu, X. (2014), "Seismic performance and collapse prevention of concrete-filled thin-walled steel tubular arches", *Thin-Wall. Struct.*, **80**(1), 91-102.

Mirza, O. and Uy, B. (2011), "Behaviour of composite beam–column flush end-plate connections subjected to low-probability, high-consequence loading", *Eng. Struct.*, **33**(2), 647-662.

Mohammad, R.S. (1999), "Modeling of bond-slip in steel-concrete composite beams and reinforcing bars", Ph.D. Dissertation; University of Colorado, CO, USA.

Nie, J.G. (2005), *Test, Theory and Application of Steel- Concrete Composite Beam*, Science Press, Beijing, China. [In Chinese]

Nie, J.G. and Cai, C.S. (2003), "Steel-concrete composite beams considering shear slip effects", *J. Struct. Eng.*, **129**(4), 495-506.

Johnson, R.P. (1994), *Composite Structures of Steel and Concrete*, Blackwell Scientific, Oxford, UK.
Kim, S.H., Jung, C.Y. and Ahn, J.H. (2011), “Ultimate strength of composite structure with different degrees of shear connection”, *Steel Compos. Struct., Int. J.*, **11**(5), 375-390.
Ollgaard, J.G., Roger, G.S. and John, W.F. (1971), “Shear strength of stud connectors in lightweight and normal-weight concrete”, *AISC Eng. J.*, **8**(2), 55-64.
Salari, MR. (1999), “Modeling of bond-slip in steel-concrete composite beams and reinforcing bars”, Ph.D. Dissertation; University of Colorado at Boulder, CO, USA.
Selçuk, E.G. and Metin, H. (2013), “Ultimate behavior of composite beams with shallow I-sections”, *Steel Compos. Struct., Int. J.*, **14**(5), 493-509.
Souici, A., Berthet, J.F., Li, A. and Rahal, N. (2013), “Behaviour of both mechanically connected and bonded steel-concrete composite beams”, *Eng. Stuct.*, **49**(4), 11-23.
Tao, M.X. and Nie, J.G. (2014), “Fiber beam-column model considering slab spatial composite effect for nonlinear analysis of composite frame systems”, *J. Struct. Eng.* **140**(1), 896-912.
Vasdravellis, G., Uy, B. and Kirkland, B. (2015), “Behaviour and design of composite beams subjected to sagging bending and axial compression”, *J. Construct. Steel Res.*, **110**(7), 29-39.
Wang, Q.T. and Chang, X. (2013), “Analysis of concrete-filled steel tubular columns with T shaped cross section”, *Steel Compos. Struct., Int. J.*, **15**(1), 41-55.
Zhao, H.L., Yu, Y. and Ye, Z.M. (2012), “Simplified nonlinear simulation of steel-concrete composite beams”, *J. Construct. Steel Res.*, **71**(4), 83-91.
Zhou, W.B., Li, S.J. and Jiang, L.Z. (2015), “Distortional buckling calculation method of steel-concrete composite box beam in negative moment area”, *Steel Compos. Struct., Int. J.*, **19**(5), 1203-1219.
Zhou, W.B., Li, S.J. and Huang, Z. (2016), “Distortional buckling of I-steel-concrete composite beams in negative moment area”, *Steel Compos. Struct., Int. J.*, **20**(1), 57-70.

CC